IOPscience iopscience.iop.org

Home Search Collections Journals About Contact us My IOPscience

Optical and electrical characteristics of a-GaAs and a-AlGaAs prepared by radio-frequency sputtering

This article has been downloaded from IOPscience. Please scroll down to see the full text article.

1990 J. Phys.: Condens. Matter 2 8063

(http://iopscience.iop.org/0953-8984/2/40/006)

View the table of contents for this issue, or go to the journal homepage for more

Download details:
IP Address: 171.66.16.151
The article was downloaded on 11/05/2010 at 06:54

Please note that terms and conditions apply.

J. Phys.: Condens. Matter 2 (1990) 8063–8074. Printed in the UK

Optical and electrical characteristics of a-GaAs and a-AlGaAs prepared by radio-frequency sputtering

M I Manssor and E A Davis
Department of Physics, University of Leicester, Leicester LE1 7RH, UK

Received 21 March 1990, in final form 3 July 1990

Abstract. Amorphous films of GaAs have been prepared by radio-frequency sputtering in an argon plus hydrogen plasma. The optical gap and refractive index have been determined as a function of hydrogen content. Vibrational modes in the infrared have also been identified. The temperature dependence of the DC electrical conductivity has been measured for films with and without hydrogen and as a function of annealing.

Co-sputtering of Al and GaAs has been used to produce a-GaAlAs films with various concentrations of Al. The electrical and optical properties of these films have also been measured. An interesting result is that the optical gap decreases with increasing Al content, in contrast to c-GaAlAs for which the gap increases. We attribute this result to the presence of 'wrong bonds'.

1. Introduction

Numerous studies have been devoted to crystalline gallium arsenide (c-GaAs) and gallium aluminium arsenide (c-$Ga_{1-x}Al_xAs$) because of their many applications in devices e.g. semiconductor lasers, light emitting diodes, etc. On the other hand fewer studies have been devoted to amorphous GaAs and, as far as we know, no one has studied GaAlAs in the amorphous form.

Selected energy gaps can be obtained in the mixed crystal system GaAs:AlAs. Junctions formed between $Ga_{1-x}Al_xAs$ and GaAs are of great importance for many optoelectronic devices, because of the small difference in lattice parameter between c-GaAs and c-$Ga_{1-x}Al_xAs$ (less than 0.15% at 300 K), leading to an insignificant concentration of undesirable interface states. The bandgap energy in c-$Ga_{1-x}Al_xAs$ as a function of the alloy composition is an important device parameter; it varies according to the relations $E_g/\text{eV} = 1.424 + 1.247x (0 < x < 0.45)$ and $1.900 + 0.125x + 0.143x^2$ $(0.45 < x < 1.0)$ [1].

Previous work has been performed on a-GaAs thin films prepared by various techniques: flash evaporation [2, 3], glow discharge [4], RF sputtering [5, 6, 7], and plasma-enhanced chemical transport deposition (PECTD) [8].

The primary objective of this work is to make a comparative study of amorphous versus crystalline GaAs and $Ga_{1-x}Al_xAs$. In this paper, we report the preparation and characterization of amorphous films of these alloys deposited by sputtering in an argon/hydrogen mixture. Optical, electrical and infrared investigations have been made. A surprising result is that the bandgap of GaAs decreases on alloying with Al.

0953-8984/90/408063 + 12 $03.50 © 1990 IOP Publishing Ltd

2. Sample preparation and characterization

Amorphous GaAs films were prepared by radio-frequency (13.56 MHz) sputtering using a 2 inch diameter single-crystal GaAs target in an atmosphere of argon and hydrogen. The relative flow rates of the two gases, and hence their partial pressures, were adjusted to vary the content of hydrogen in the film. The base pressure was about 1.5×10^{-7} Torr (2×10^{-5} Pa) and the total chamber pressure during the sputtering was 6.5 mTorr (0.86 Pa). A residual-gas analyser (mass spectrometer) established the absence of any appreciable contaminants such as CO_2 and H_2O in the system. The RF power applied to the target was 70–80 W. The films were deposited simultaneously on various ultrasonically cleaned substrates, including 7059 Corning glass for optical and electrical measurements, mica for transmission electron microscope (TEM) measurements and c-Si for infrared spectroscopy. The target to substrate separation was 5.5 cm, and the substrate was held at about 20 °C by water cooling.

Amorphous GaAlAs films were prepared in a similar way to a-GaAs. The aluminium content of the film was altered by varying the number and area of aluminium chips on the GaAs target.

The composition of the samples was determined by energy-dispersive x-ray analysis using a D.S.130 SEM. The resulting films were As rich compared to stoichiometric $(GaAs)_{1-x}Al_x$ as shown in figure 1. The tie lines of $(GaAs)_{1-x}Al_x$ and $(Ga_{1-x}Al_x)As$ are also shown. A few % of Ar was detected in some of the samples; hydrogen cannot be detected by this technique. These measurements also confirmed the homogeneity of the films.

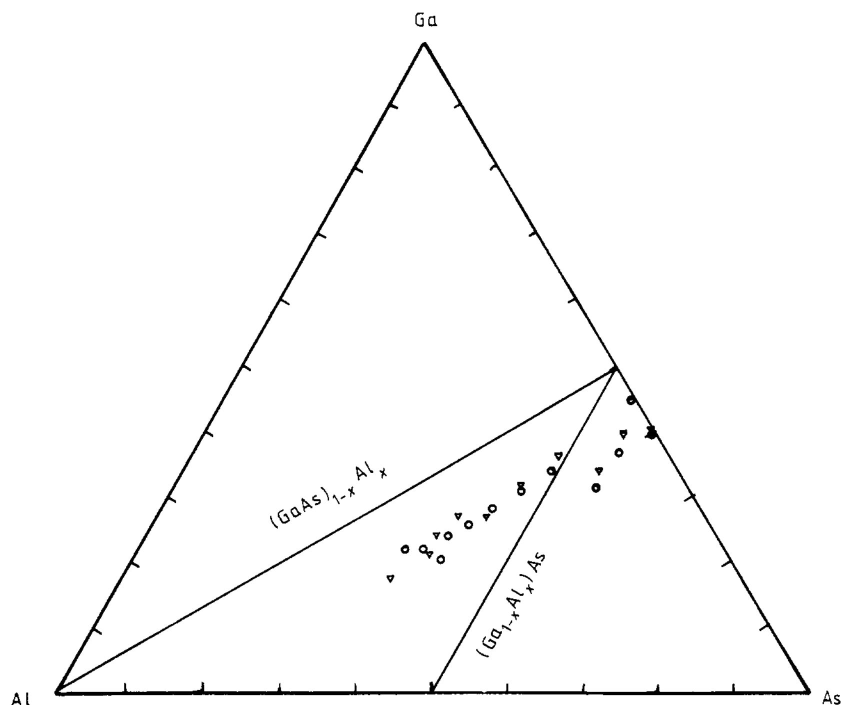

Figure 1. Composition of the samples used in this investigation (○, hydrogenated; △, unhydrogenated GaAlAs films).

The thickness d of the films was measured using a Talysurf profiler and also an optical method [9] using reflectance and transmittance data over a range of wavelengths. Good agreement was obtained for the values of d measured by both methods. They were in the range 0.20–1.0 μm.

Evidence for the amorphous structure was obtained using a TEM. The films for these experiments were deposited on to mica with a thickness of about 400 Å. The deposited film was floated off in distilled water. The pieces of film were then gently lifted out of the water using a standard copper electron microscope grid. All GaAs samples examined were amorphous while those of GaAlAs were amorphous up to about 30 at.% of Al but exhibited a polycrystalline structure above this concentration.

3. Optical and electrical measurements on a-GaAs(:H)

3.1. Refractive index of a-GaAs(:H)

The index of refraction, n, was obtained from examination of the minima and maxima of interference fringes in reflection to determine their order m. Now $n = m\lambda_m/4d$ [9], where λ_m is the wavelength at the mth minimum or maximum and d is the measured thickness. Since m is a small integer, it can be determined without error; incorrect values for m lead to unreasonable values for n. Thus, knowing d, m and the wavelength of the corresponding fringes, it is possible to determine n as a function of wavelength.

Figure 2 presents the refractive index, n, as a function of photon energy for differently hydrogenated samples. The refractive index at 0.5 eV for an unhydrogenated a-GaAs film is of the order of 3.7. This can be compared with the refractive index obtained by Gheorghiu and Theye [2] for stoichiometric films deposited at low temperature (100 K) for which n was of the order of 3.8. In figure 2 and subsequent figures, 'increasing hydrogen content' refers to larger flow rates of hydrogen relative to argon through the chamber during sputtering; the actual hydrogen content in the films is not known but it is clear from infrared spectra (to be reported below) that the hydrogen content increases with the flow rate. For the purposes of comparison the refractive index of high-purity c-GaAs is also included in the figure [10]. We can observe that at a fixed photon energy the refractive index of the amorphous films decreases with increasing hydrogen content,

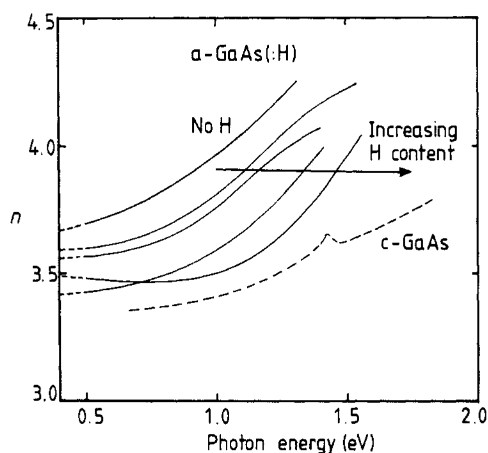

Figure 2. Refractive index versus photon energy for various a-GaAs(:H) films.

and that it increases with photon energy as the fundamental absorption edge is approached. In contrast to c-GaAs, the refractive index for a-GaAs does not show any peak at the bandgap energy where the absorption coefficient changes rapidly.

3.2. Optical absorption edge of a-GaAs(:H)

The absorption coefficient was determined from measurements of transmittance T and reflectance R, for wavelengths ranging between 400 and 2500 nm, using a double-beam Perkin-Elmer 330 spectrophotometer. The absorption coefficient was obtained from the expression [11]

$$T = (1 - R_1)(1 - R_2)(1 - R_3)\exp(-\alpha d)/(1 - R_2R_3)\{1 - [R_2R_2 + R_1R_3(1 - R_2)^2]\exp(-2\alpha d)\} \quad (1)$$

where R_1, R_2, R_3 are the reflectivities of the air-film, film-substrate and substrate-air interfaces. When αd is small ($\ll 1$) the imaginary part of the refractive index is negligible and

$$R_1 = (n - n_a)^2/(n + n_a)^2 \quad (2a)$$

$$R_2 = (n - n_s)^2/(n + n_s)^2 \quad (2b)$$

$$R_3 = (n_s - n_a)^2/(n_s + n_a)^2 \quad (2c)$$

where n_a is the refractive index of air ($n_a = 1$), n_s is the refractive index of the substrate ($n_s = 1.53$), and n is the refractive index of the film. The following approximate expression was used in the high absorption region [12]

$$T = (1 - R_m)\exp(-\alpha d) \quad (3)$$

where $T = I_T/I_0$ is the transmittance, $R_m = I_R/I_0$ is the measured reflectance, I_T and I_R are the total transmitted and reflected intensities and I_0 is the incident beam intensity. The absorption coefficient as a function of energy for the low- and high-absorption regions overlapped and matched well using the two expressions.

Figure 3 shows the absorption coefficient of a-GaAs:H as a function of photon energy for different H/Ar flow ratios. For comparison we have plotted the variation for c-GaAs [13]. The optical energy gap (Tauc gap) E_T was determined from the Tauc law [14]

$$\alpha h\omega = \text{constant}\,(h\omega - E_T)^2. \quad (4)$$

The Tauc plots obtained from the experimental data of figure 3, are displayed in figure 4. The optical gap of the unhydrogenated a-GaAs film shown in figure 4 is of the order of 1.0 eV. This compares favourably with values (1.0–1.1 eV) obtained by others for films prepared by different methods [2–8]. Our films are As-rich (see figure 1) but results [3] on films containing an excess of As show that the optical gap is not too sensitive to composition variations near stoichiometry. It is evident that with increasing hydrogen content the absorption edge shifts towards higher energy and E_T increases.

3.3. Dark DC *conductivity of a-GaAs(:H)*

The electrical conductivity was measured by either a four- or two-probe technique using a Keithley 616 digital electrometer and a Keithley 181 digital nanovoltmeter. Gold

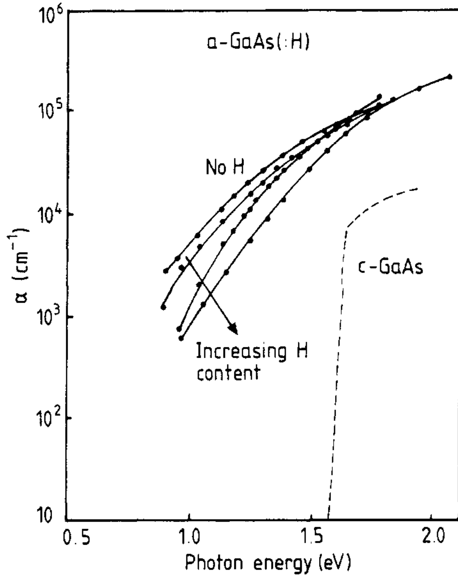

Figure 3. Absorption coefficient α versus photon energy for a-GaAs prepared with different H/Ar flow rate ratios.

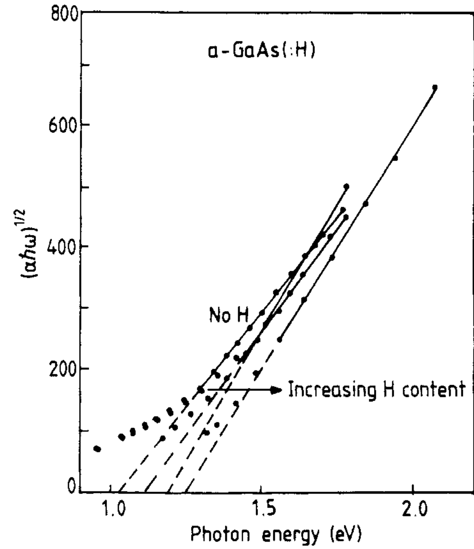

Figure 4. Tauc plot for a-GaAs(:H) films as a function of photon energy for various H/Ar flow rate ratios.

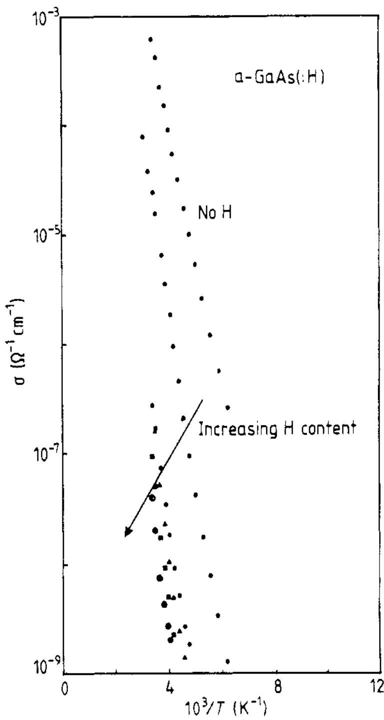

Figure 5. Log σ versus $1/T$ for several a-GaAs(:H) films below room temperature.

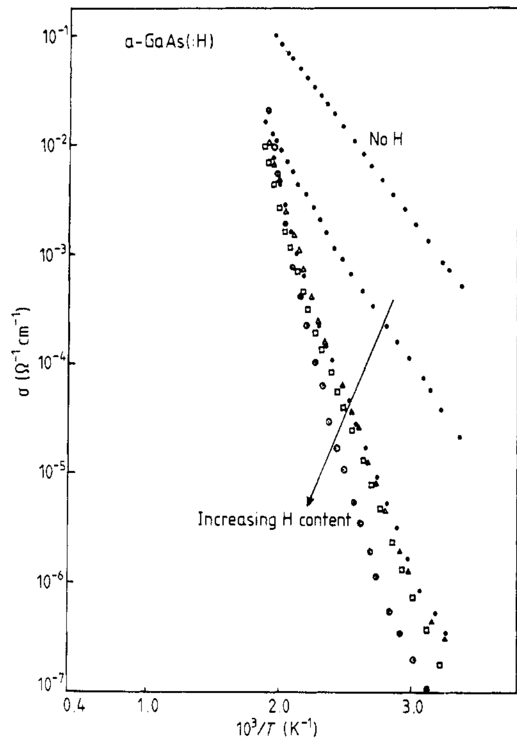

Figure 6. Log σ versus $1/T$ for several a-GaAs(:H) films above room temperature.

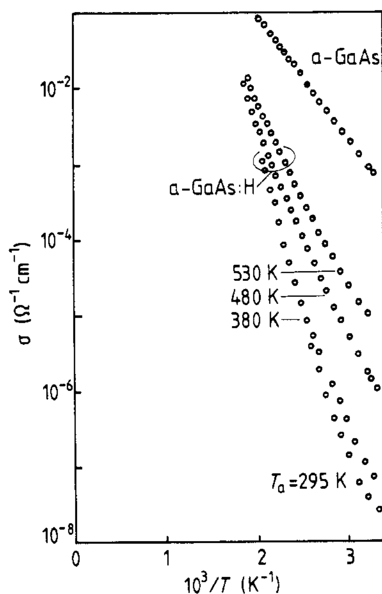

Figure 7. Log σ versus $1/T$ for an a-GaAs : H film annealed at different temperatures T_a. The curve marked a-GaAs contains no hydrogen. Anneal time 1 hour at each anneal temperature.

electrodes 1.2 cm long and 4 mm apart were evaporated in a co-planar configuration onto the samples.

The temperature dependence of the conductivity, σ, (for temperatures below room temperature) of a-GaAs(:H) films prepared with various hydrogen concentrations is shown in figure 5. With increasing H content, the conductivity decreases and the activation energy E_a increases. Figure 6 shows similar results above room temperature. The activation energies, calculated over the temperature range 300–360 K, are approximately equal to half the optical gap, suggesting a Fermi level pinned near mid-gap.

It can be seen in figure 6 that, for hydrogenated a-GaAs, the conductivity curves bend upwards above 430 K. This seems likely to be associated with evolution of hydrogen from the samples at the higher temperatures [15]. In order to investigate hydrogen evolution we measured the conductivity of a hydrogenated sample as a function of annealing in vacuum for periods of one hour at several temperatures T_a. It was found that (i) the conductivity at room temperature increased and (ii) the activation energy decreased as shown in figure 7, the curves approaching that for unhydrogenated a-GaAs also shown in the figure. Table 1 shows the affect of annealing on σ and E_a at different annealing temperatures.

These observations were supported by infrared measurements carried out on a film deposited under exactly the same conditions (in the same run) deposited on c-Si. The film was annealed at identical temperatures to those for the conductivity measurements. It was found that a broad band at 1460 cm^{-1}, which is believed to be a hydrogenic mode (see next section), flattened out.

Table 1

Annealing T (K)	295	380	480	530
σ_{RT} (Ω^{-1} cm^{-1})	3.8×10^{-8}	9.0×10^{-8}	1.7×10^{-6}	1.0×10^{-5}
E_a (eV)	0.61	0.58	0.50	0.43

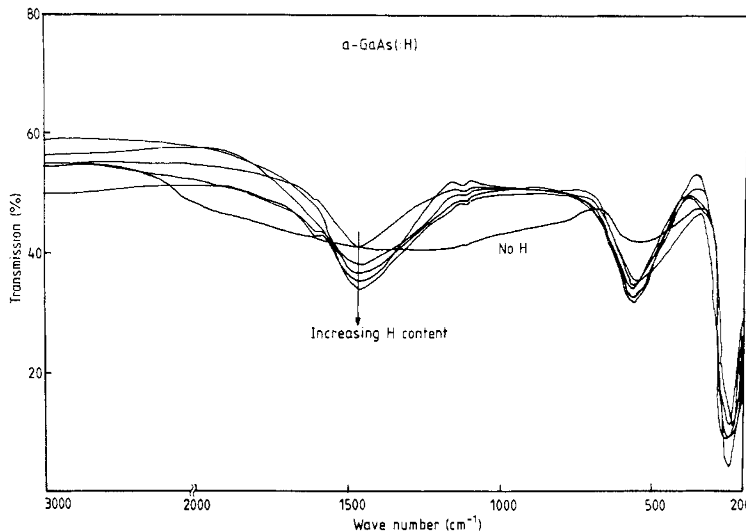

Figure 8. Infrared transmission spectra of a-GaAs(:H) films prepared with different H/Ar flow rate ratios.

3.4. Infrared measurements on a-GaAs(:H)

The infrared transmission spectra from 4000 cm^{-1} to 200 cm^{-1} of a set of samples of a-GaAs(:H), deposited on c-Si substrates at different H/Ar flow ratios, were measured with a Perkin-Elmer model 580B double-beam spectrophotometer with a blank c-Si substrate in the reference beam. Three strong absorption bands were observed at 1460 cm^{-1}, 530 cm^{-1} and 250 cm^{-1} as shown in figure 8. Paul *et al* [15] have pointed out that the two strong broad bands at 1460 and 530 cm^{-1} are hydrogenic modes, and Wang *et al* [16] assigned them to Ga–H–Ga bridge stretching and wagging modes respectively.

4. Optical and electrical measurements on a-GaAlAs(:H)

4.1. Optical absorption edges of a-GaAlAs(:H)

The optical absorption coefficient α for a-GaAlAs was calculated from the relation

$$T = (1 - R_m)^2 \exp(-\alpha d)/[1 - R_m^2 \exp(-2\alpha d)] \quad (5)$$

i.e.

$$\alpha d = \ln\{(1 - R_m)^2/2T + [(1 - R_m)^4/4T^2 + R^2]^{1/2}\} \quad (6)$$

where R_m is the measured reflectivity and d is the thickness of the film. Equation (6) allows αd to be calculated and, knowing the thickness d, one can determine α. It was not possible to use equation (1) to determine α in a-GaAlAs because of the absence of interference fringes, especially at high Al concentrations, making it difficult to determine R_1 and R_2 in terms of refractive indices.

Figure 9 shows, respectively, the absorption coefficients for hydrogenated and unhydrogenated a-GaAlAs as a function of photon energy for various Al concentrations. It can be seen from the figure that the absorption edge shifts towards lower energy and

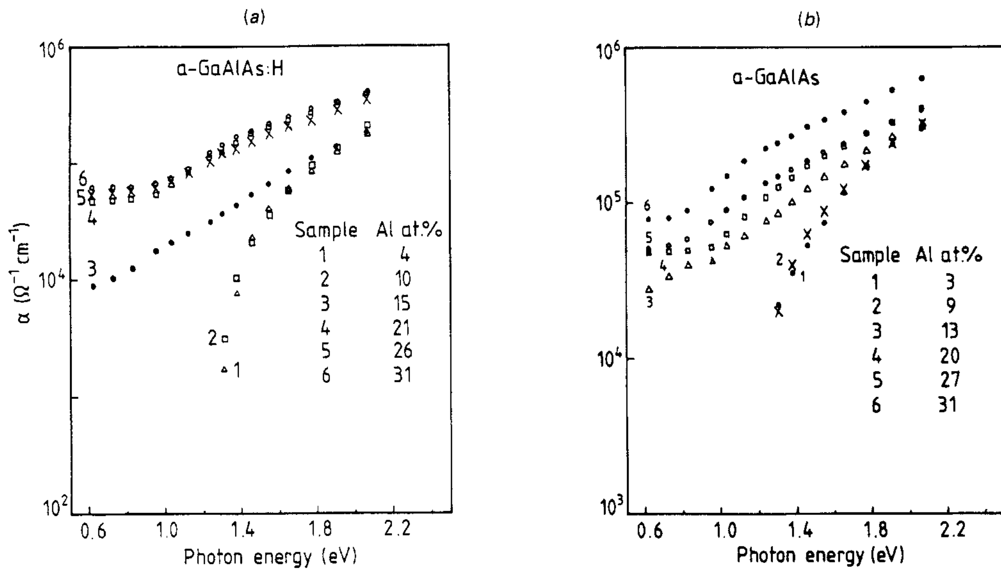

Figure 9. Absorption coefficient α versus photon energy of films for various Al concentration (*a*) A-GaAlAs : H. (*b*) a-GaAlAs.

broadens with Al addition. At low photon energies and high Al content the edge becomes nearly flat. The reason for this behaviour is not clear, but is probably associated with Al-related defect states in the gap.

The optical energy gap E_T was determined from the Tauc law [14] (equation (4)). Tauc plots obtained from experimental data in figure 9(*a*) are displayed in figure 10. The variations of E_T with Al concentration for both hydrogenated and unhydrogenated a-GaAlAs are shown in figure 11. This curve can be divided into two regions. In region 1

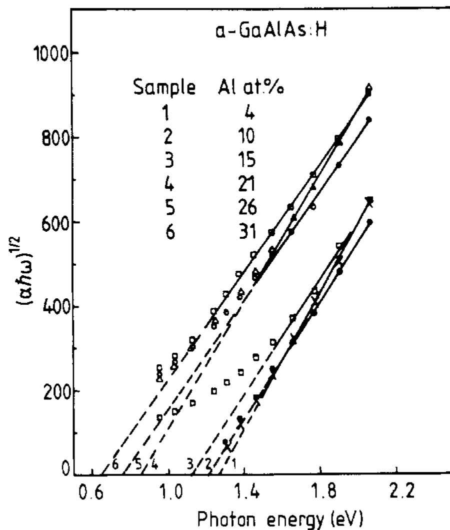

Figure 10. Tauc plot for a-GaAlAs : H versus photon energy for various Al concentrations.

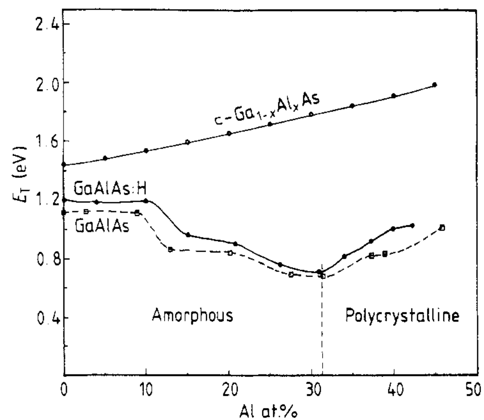

Figure 11. Dependence of the optical gap E_T on the Al content of GaAlAs.

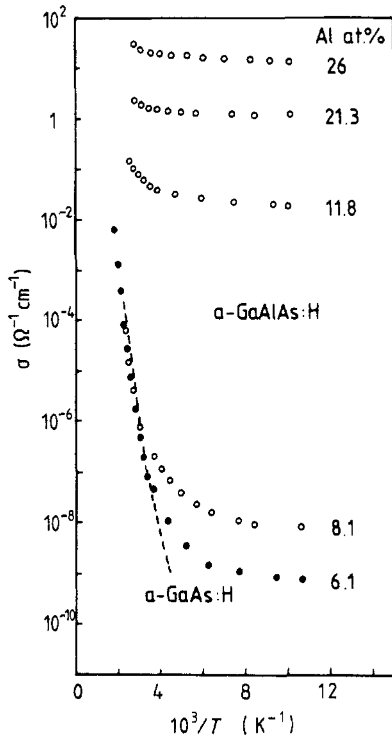

Figure 12. Log σ versus $1/T$ for a series of films of a-GaAlAs:H.

(Al content <31 at.%) E_T remains roughly constant for Al content less than 8 at.% but decreases for Al content above this value, while in region 2 (Al content >31 at.%) E_T increases with increasing Al content. As pointed out earlier (section 2), the films in these two regions have different structures; amorphous and polycrystalline respectively. Figure 11 also shows the variation of the optical gap in crystalline $Ga_{1-x}Al_xAs$ [1] and will be referred to in section 5.

4.2. Dark DC *conductivity of a-GaAlAs(:H)*

The temperature dependence of the conductivity σ of the samples with various Al concentration is shown in figure 12. It can be seen that with increasing Al content the conductivity rises, particularly when the Al content is increased from about 8.1 to 11.8 at.% Al. The high-temperature activation energies for a-GaAs:H and for a-GaAlAs:H with 6.1 and 8.1 at.% Al are all about 0.6 eV. Comparison with figure 11 shows that the optical gap is approximately equal to $2E_a$ for these samples and one can conclude that the Fermi energy is pinned close to mid-gap. At lower temperatures and for higher Al content, the conductivity is only weakly dependent on temperature, suggesting a mechanism of conduction by hopping in localized states near the Fermi energy.

4.3. Infrared measurements of GaAlAs(:H)

Figure 13 shows infrared transmission spectra for five unhydrogenated GaAlAs samples. Figure 14 shows the transmission spectra of hydrogenated GaAlAs samples with similar Al concentration. It can be seen that by adding Al to a-GaAs, the band at about 250 cm^{-1}

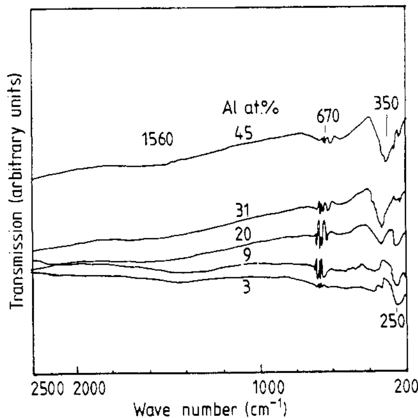

Figure 13. IR transmission for a series of films of GaAlAs.

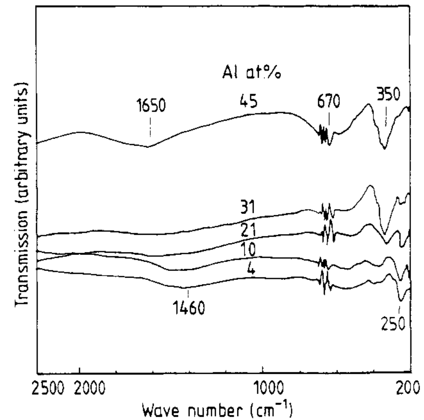

Figure 14. IR transmission for a series of films of GaAlAs:H.

shifts to about 350 cm^{-1} for 31 and 45 at.% Al content. In addition, two broad absorption bands, at 600–700 cm^{-1} and near 1600 cm^{-1} appear. In the hydrogenated samples (figure 14), these two bands are stronger and one can determine their centre frequencies to be about 670 cm^{-1} and 1650 cm^{-1}. We have already mentioned (section 3.4) that Ga–H–Ga bridge wagging and stretching modes occur at 530 and 1460 cm^{-1} respectively [16]. Bridging hydrogen has been found in a number of aluminium compounds (Al–H–Al bridges) such as $Al(BH_4)_2H$ and $Al(BH_4)H_2$ [17]. In these compounds, the Al–H–Al stretching vibrations have been reported to occur in a broad band between 1200 and 2200 cm^{-1}, centred near 1650 cm^{-1}. The Al–H–Al wagging modes lie between 470 and 1050 cm^{-1} with a maximum at 730 cm^{-1}. So the broad band centred near 1650 cm^{-1} in our films can be assigned as an Al–H–Al stretching mode and that at 670 cm^{-1} to a wagging band. The shifts to higher wavenumbers in going from Ga–H bonds to Al–H bonds are reasonable in view of the difference in the covalent radii r_c (r_c for Ga is 1.26 Å and that for Al is 1.18 Å) since the vibration frequency is approximately proportional to $r_c^{-1.5}$ [16].

5. Discussion and summary

The optical measurements on a-GaAs films showed that the absorption edge of these films shifts towards higher energies with hydrogen incorporation becoming closer to that of c-GaAs. A similar shift and accompanying sharpening of the edge is observed for a-Si:H. The generally accepted reasons for the effect of hydrogen in increasing the gap of amorphous silicon are (i) a recession of the top of the valence band by replacement of weak Si–Si bonds with stronger Si–H bonds and (ii) the removal of mid-gap dangling-bond states by hydrogen bonding to threefold coordinated (Si_3) silicon atoms [18]. It should also be noted that the smallest gap in c-Si is indirect and relaxation of the k-selection rule leads, irrespective of the hydrogen content, to a larger gap in a-Si:H.

In c-GaAs the smallest gap is direct and so no similar shift associated with k relaxation in a-GaAs is expected. However, Ga and As dangling bonds (Ga_3 and As_3) are expected in the amorphous phase. Robertson [19] has calculated that the unrelaxed Ga_3 level lies just below the conduction band edge while the As_3 level lies near the valence band.

Hydrogen incorporation probably satisfies these dangling bonds, eliminating the associated states from the gap. Antisite or wrong (i.e. Ga–Ga and As–As) bonds also give states around the band edges [19]. Our infrared measurements on the same samples confirm the presence of Ga–H–Ga bonds in the hydrogenated samples (figure 8) and we suggest that these form at the expense of Ga–Ga bonds.

Annealing the a-GaAs : H samples increased their conductivities towards the value of unhydrogenated samples, and also causes a Ga–H–Ga band in the IR spectra to disappear when annealed to 530 K. This is attributed to the evolution of incorporated hydrogen in the film with a consequent rearrangement of the network.

Conductivity measurements on the a-GaAs(:H) film above room temperature showed an activated behaviour characteristic of band-like conduction in extended states. The activation energy is of the order of half the optical gap; this therefore suggests that the Fermi level is located approximately at mid-gap.

The reason for a decrease in energy gap with increasing Al concentration in a-GaAlAs(:H) films, in contrast to an increase in c-$Ga_{1-x}Al_xAs$, is not very clear.† However, one can argue that, in c-$Ga_{1-x}Al_xAs$, Al is substitutionally incorporated in place of Ga atoms and only bonds between Ga–As or Al–As are expected. Wrong bonds have low probability of occurrence in this crystalline system. The energy gap in c-AlAs is higher than that for c-GaAs and increases monotonically with Al content. However, the situation is quite different in the a-GaAlAs(:H) system. Wrong bonds are expected in non-stoichiometric GaAs [19] and we expect them also in the ternary compound. Each Al atom will not necessarily substitute for a Ga atom in such a random network and therefore like-atom or wrong bonds are expected (e.g. Ga–Ga, Al–Al, As–As, and Ga–Al). This may be a possible explanation for the decrease of the energy gap with Al alloying. EXAFS studies are underway to determine the bonding configurations in the amorphous materials with a view to testing this suggestion.

For concentrations of Al higher than 30 at.%, the films are polycrystalline and the trends in the optical gap are then in the same direction as for crystalline GaAlAs.

Acknowledgments

The authors would like to thank S C Bayliss, R A Asal, A Singh, H S Derbyshire and S H Baker for assistance and discussions relating to this work. We also wish to thank G McTurk and C D'Lecey for composition and TEM measurements. M I Manssor acknowledges the Ministry of Higher Education and Scientific Research, Iraq, for providing a scholarship.

References

[1] Casey H C Jr and Panish M B 1978 *Heterostructure Lasers* (New York: Academic) part A
[2] Gheorghiu A and Theye M L 1981 *Phil. Mag.* B **44** 285
[3] Theye M L, Gheorghiu A, Driss-Khodja K and Boccara C 1985 *J. Non-Cryst. Solids* **77–78** 1293
[4] Segui Y, Carrere F and Bui A 1982 *Thin Solid Film* **92** 303
[5] Alimoussa L, Carchano H and Thomas J P 1981 *J. Physique Coll. Suppl.* 10 **42** C4 683

† It should be emphasized that the comparison of the variations of E_T with Al content for amorphous and crystalline forms shown in figure 11 is not strictly valid. Data for the crystalline form [1] refer to compositions along the $(Ga_{1-x}Al_x)As$ tie line (see figure 1) where our amorphous samples intersect this line but lie parallel to the $(GaAs)_{1-x}Al_x$ tie line.

[6] Paul W, Moustakas T D, Anderson D A and Freeman E 1977 *Proc. Int. Conf. on Amorphous and Liquid Semiconductors* ed W E Spear (Centre of Industrial Consultancy and Liaison, University of Edinburgh), p 467
[7] Bandet J, Frandon J and Bacque G 1988 *Phil. Mag.* B **58** 645
[8] Chen Kun-ji, Yang Zuo-Ya and Wu Ru-Ling 1985 *J. Non-Cryst. Solids* **77–78** 1281
[9] Cisneros J J, Rego G B, Tomyiama M, Bilac S, Goncalves J M, Rodriguez A E and Arguello Z P 1983 *Thin Solid Films* **100** 155
[10] Casy H C Jr, Sell D D and Panish M B 1974 *Appl. Phys. Lett.* **24** 63
[11] Brodsky M J, Title R S, Weiser K and Pettit G D 1970 *Phys. Rev.* B **1** 2633
[12] Al-Sharbaty A 1974 *Ph.D Thesis* University of Dundee
[13] Sze S M 1981 *Physics of Semiconductor Devices* (New York: Wiley)
[14] Tauc J 1972 *Optical Properties of Semiconductors* (Amsterdam: North-Holland)
[15] Paul D K, Blake J, Oguz S and Paul W 1980 *J. Non-Cryst. Solids* **35–36** 501
[16] Wang Z P, Ley L and Cardona M 1982 *Phys. Rev.* B **26** 3249
[17] Oddy P R and Wallbridge M G H 1978 *Chem. Soc. Dalton* 572
[18] Roedern B Von, Ley L and Cardona M 1977 *Phys. Rev. Lett.* **39** 1576
[19] Robertson J 1985 *J. Non-Cryst. Solids* **77–78** 37